

# Two nuclear localization signals regulate intracellular localization of the Duck enteritis virus UL13 protein

**Linjiang Yang**

Sichuan Agriculture University

**Xixia Hu**

Sichuan Agriculture University

**Anchun Cheng** (✉ [chenganchun@vip.163.com](mailto:chenganchun@vip.163.com))

Sichuan Agricultural University <https://orcid.org/0000-0001-6093-353X>

**Mingshu Wang**

Sichuan Agriculture University

**Renyong Jia**

Sichuan Agriculture University

**Qiao Yang**

Sichuan Agriculture University

**Ying Wu**

Sichuan Agriculture University

**Shun Chen**

Sichuan Agriculture University

**Mafeng Liu**

Sichuan Agriculture University

**Dekang Zhu**

Sichuan Agriculture University

**Xumin Ou**

Sichuan Agriculture University

**Xingjian Wen**

Sichuan Agriculture University

**Sai Mao**

Sichuan Agriculture University

**Di Sun**

Sichuan Agriculture University

**Shaqiu Zhang**

Sichuan Agriculture University

**Xinxin Zhao**

Sichuan Agriculture University

**Juan Huang**

Sichuan Agriculture University

**Qun Gao**

Sichuan Agriculture University

**Yunya Liu**

Sichuan Agriculture University

**Yanling Yu**

Sichuan Agriculture University

**Ling Zhang**

Sichuan Agriculture University

**Bin Tian**

Sichuan Agriculture University

**Leichang Pan**

Sichuan Agriculture University

**Mujeeb Ur Rehman**

Sichuan Agriculture University

**Xiaoyue Chen**

Sichuan Agriculture University

---

**Research article**

**Keywords:** Duck enteritis virus; Conserved herpesvirus protein kinase; UL13; NLS

**Posted Date:** March 20th, 2020

**DOI:** <https://doi.org/10.21203/rs.3.rs-15523/v2>

**License:** © ⓘ This work is licensed under a Creative Commons Attribution 4.0 International License. [Read Full License](#)

---

**Version of Record:** A version of this preprint was published at Poultry Science on January 1st, 2021. See the published version at <https://doi.org/10.1016/j.psj.2020.09.069>.

## Abstract

Background UL13 multifunctional tegument protein duck enteritis virus (DEV) is predicted as conserved herpesvirus protein kinase (CHPK); however, little is known about its subcellular localization signal. Results In this study, by transfection with two predicted nuclear signals of DEV UL13 fused to enhanced green fluorescent protein (EGFP), two bipartite nuclear localization signals (NLS) were identified. We found that the NLSs block its nuclear import using ivermectin and proved that nuclear localization signal of DEV UL13 is a classical importin  $\alpha/\beta$ -dependent process. And we constructed the DEV UL13 mutant strain, with the NLSs of DEV UL13 deleted, to explore whether it can affect the virus replication. Conclusions The DEV pUL13 amino acids 4 to 7 and 90 to 96 was predicted, and proved that this nuclear import occurs via the classical importin  $\alpha/\beta$ -dependent process. We also found NLSs of pUL13 have no effect on DEV replication in cell culture. Our study enhances the understanding of DEV pUL13. Taken together, these results would provide significant information for the biological function of pUL13 during DEV infection.

## Background

Duck enteritis virus (DEV), a member of the alphaherpesvirinae subfamily, can cause serious clinical symptoms and pathological changes, such as vascular injury, tissue haemorrhage, gastrointestinal mucosal papulosis-like lesions, and degeneration of lymphoid and parenchymal organs [1–3]. Also, DEV can lead to acute, fever, septicaemia and infectious diseases in ducks, geese, swans and other birds. The morbidity and mortality of infected or unprotected ducks are as high as 100 %. This disease often trigger severe economic losses to the global waterfowl industry [4].

According to the Ninth International Committee on Taxonomy of Viruses (ICTV), DEV is classified into the subfamily alphaherpesvirinae of the Herpesviridae [5]. DEV infection, known as duck plague (DP) or duck viral enteritis (DVE), is among the most widespread and devastating diseases of waterfowl [6]. DEV is a linear double-stranded DNA virus that contains 78 open reading frames. The UL13 gene of DEV, which is predicted to encode a Ser/Thr conserved herpesvirus protein kinase (CHPK), was previously identified by our team [7-8]. Amino acid sequence analysis found that the pUL13 kinase shows more than 35% similarity with reported CHPK, and the exploration of DEV UL13 will not only provide information about the molecular biological characteristics of DEV but also promote the knowledge of the CHPK family.

CHPKs can autophosphorylate and phosphorylate certain viral and cellular proteins that help the virus replicate and spread, with many activities occurring in the nucleus. For example, CHPKs have been reported to participate in the phosphorylation of nuclear lamina components to facilitate the nuclear egress of progeny capsids [9-14]. In addition to take part in nuclear egress, CHPKs have been proven to influence viral replication and the cell cycle. CHPKs affect virus replication by phosphorylating DNA polymerase processivity factors, such as UL44 of human cytomegalovirus (HCMV) and BMRF1 of Epstein-Barr virus (EBV) [15, 16], histones [17], and RNA polymerase II [18, 19], to promote viral DNA replication and protein expression. In recent years, the EBV BGLF4 protein has been demonstrated to inhibit cell cycle G1/S progression and induce chromosomal abnormality [20, 21]. Moreover, herpes simplex virus 1 (HSV-1) pUL13 has been found to stimulate the expression of suppressor of cytokine signalling 3 (SOCS-3), a negative regulator of IFN, to escape the interferon response. It has also been reported that CHPKs of HCMV, EBV, Kaposi's sarcoma-associated herpesvirus (KSHV), and murine herpesvirus-68 (MHV-68) can subvert the type I IFN response by inhibiting the activity of interferon regulatory factor 3 (IRF-3) [22-24].

Furthermore, some, but not all, CHPKs in betaherpesvirinae and gammaherpesvirinae can phosphorylate antiviral nucleoside analogue ganciclovir (GCV) [25-29], which is also present in the nucleus.

The characteristics of some genes from DEV had been reported by our team [30-56]. However, the function of DEV UL13 protein has rarely been reported to date. Some of the DEV pUL13 characteristics have been identified in our previous study. This report will complement the location characteristic of DEV UL13 and lay the foundation for its functional exploration in the nucleus.

## Results

### Localization of recombinant UL13 and UL13- $\Delta$ NLSs mutated protein in transfected DEFs

We have determined that DEV pUL13 also can enter into the nucleus. PSORT II prediction revealed amino acids 4 to 7 (Arg-Arg-Arg-Arg) and 90 to 96 (Pro-Gly-Lys-Arg-Lys-Thr-Lys), as putative NLSs (Figure S1). To examine the function of these predicted NLSs, we constructed expression plasmids for UL13-GFP fusion proteins or proteins with NLS1 or/and NLS2 deleted (Figure 1A) and transfected them into DEFs. Compared with that the fluorescence of UL13-GFP fusion proteins located in nucleus and cytoplasm (Figure 1B b, g, l), when NLS1 or NLS2 was deleted, the majority of the fluorescence displayed a cytoplasmic distribution in DEFs (Figure 1B c, h, m, d, i, n). Furthermore, the UL13-GFP fusion protein, with NLS1 and NLS2 both deleted, exhibited a completely cytoplasmic distribution (Figure 1B e, j, o). We also analysed the nuclear compartmentalization of UL13/UL13- $\Delta$ NLSs. As shown in Figure 1C, the nuclear/cytoplasmic fluorescence ratio of the UL13- $\Delta$ NLS1&NLS2 was significantly decreased compared to the pUL13 ( $P=0.01$ ), and both the UL13- $\Delta$ NLS1 and UL13- $\Delta$ NLS2 proteins were also significantly decreased ( $P=0.001$ ). The decrease in the nuclear/cytoplasmic fluorescence ratio was higher for UL13- $\Delta$ NLS1&NLS2 than for UL13- $\Delta$ NLS1 and UL13- $\Delta$ NLS2. All these results suggested that both NLS1 and NLS2 are responsible for the nuclear localization of DEV pUL13 and work together to enhance this function. We also separated the cytoplasmic and nuclear proteins expressed in DEF cells, and analysed the quantity of pUL13 distributed in the cytoplasm and nucleus via western blot (Figure 1D). Compared with the distribution of the DEV pUL13, the ratio of UL13- $\Delta$ NLS1 &  $\Delta$ NLS2 group was significantly reduced. We used  $\beta$ -actin and Lamin A/C as controls for these cytoplasmic/nuclear fractions in western blot and consistent with the IFA result.

### Localization of the NLS-GFP fusion protein in transfected DEFs

To further examine whether NLS1 and NLS2 can import heterologous proteins into the nucleus, sequences encoding NLS1 and NLS2 were fused to GFP to obtain NLS1-GFP, NLS2-GFP, and NLS1&NLS2-GFP recombinant plasmids and transfected into DEFs (Figure 2A). Fluorescence assays showed a greater proportion of the NLS1-GFP and NLS2-GFP fusion proteins in the nucleus than in the cytoplasm (Figure 2B b, f, j, c, g, k). In contrast, NLS1&NLS2-GFP showed a predominantly nuclear distribution (Figure 2B d, h, l) compared with GFP alone (Figure 2B a, e, i). We also analysed differences in the nuclear and cytoplasmic fluorescence ratios between GFP and NLSs-GFP and found that the nuclear/cytoplasmic fluorescence ratios for NLS1-GFP, NLS2-GFP and NLS1&NLS2-GFP were significantly increased compared to GFP ( $P=0.001$ ) (Figure 2C), with that of NLS1&NLS2-GFP being particularly increased. We also separated the cytoplasmic and nuclear proteins expressed from NLS1-GFP or NLS2-GFP plasmids in DEF cells, and analysed the quantity of UL13 protein distributed in the cytoplasm and

nucleus via western blot (Figure 2D). Compared with the distribution of the UL13 protein expressed in the nucleus, the ratio of pUL13 in the cytoplasm in the NLS1-GFP or NLS2-GFP group was significantly reduced.

Our results confirmed that both NLS1 and NLS2 of DEV pUL13 act as nuclear localization signals. Each could mediate protein entering into the nucleus, and their combination increased the function of the nuclear localization signals.

### **The effect of nuclear import inhibitors on the location of DEV UL13**

NLS1 and NLS2 of DEV UL13 are predicted to be 4 and 7 monopartite prototypical nuclear localization signals, respectively. It has been reported that ivermectin blocks importin  $\alpha$  and  $\beta$  interaction and inhibits the nuclear transport facilitated by the prototypical NLS-mediated mechanism, with no effect on proteins containing NLSs recognized by alternative nuclear import pathways. Therefore, we tested whether the nuclear import of the DEV pUL13 requires the interaction with importin  $\alpha$  and  $\beta$  by treating DEF cells transfected with UL13 recombinant plasmids with/without ivermectin. As shown in Figure 3A, less DEV pUL13 was found in nuclear in treated with ivermectin group than without ivermectin treatment at 16 h post-transfection (Figure 3A a, g, m, b, h, n). The distribution of NLS1&NLS2-GFP with ivermectin treatment in nuclear was also reduced compared to the no treatment group (Figure 3A c, i, o, d, j, p), whereas there was no change in the distribution of GFP alone with or without ivermectin treatment (Figure 3A e, k, q, f, l, r). We also analysed differences in the nuclear and cytoplasmic fluorescence ratio of NLS1&NLS2-GFP and UL13-GFP in DEF cells with or without ivermectin treatment and found that the ratio of UL13-GFP declined significantly ( $P < 0.001$ ), with the mean ratio of the NLS1&NLS2-GFP group reduced from 0.8 to 0.4 after treating with ivermectin. Statistical analysis showed that the nuclear accumulation of NLS1&NLS2-GFP and UL13-GFP was significantly impaired by ivermectin (Figure 3B) ( $P < 0.01$ ). These results suggested that the nuclear import of DEV pUL13 occurs by the classical transport process that requires the interaction of importin  $\alpha$  and  $\beta$  and is mediated by the NLSs of DEV pUL13.

### **Entry nucleus of pUL13 has no effect on DEV replication in cell culture**

To examine the effect of pUL13 entry nucleus on viral proliferation, we constructed DEV CHv-UL13 $\Delta$ NLS, which was a mutant of both NLS1 and NLS2 of DEV UL13 being deleted, and DEV CHv-UL13 $\Delta$ NLS R (a revertant) (Figure 4A). By RFLP analysis and sequencing, we determined that the DEV CHv-UL13 $\Delta$ NLS and DEV CHv-UL13 $\Delta$ NLS R recombinant viruses were mutated only at their appropriate target site (Figure 4B).

A plaque assay indicated that the DEV CHv-UL13 $\Delta$ NLS could grow in DEF, and the difference of plaque size between DEV CHv-UL13 $\Delta$ NLS and DEV CHv has no significance (Figure 5A). The growth curve of DEV CHv-UL13 $\Delta$ NLS exhibited the same trend of DEV CHv in both the supernatant and cytoplasm during the infection (Figure 5B). The phenotype of DEV CHv- $\Delta$ UL13R exhibited similar.

## **Discussion**

All herpesviruses encode serine/threonine kinases, which are involved in viral proliferation and organism immunity [57]. Two types of conserved herpesvirus serine/threonine kinases have been described in herpesviridae: one is conserved only in the alphaherpesvirus subfamily, exemplified by the US3 kinase of HSV; the others are CHPKs, which are conserved across the entire family. Studies on CHPKs have mainly focused on the function and molecular characteristics, especially for human herpesviruses, whereas studies on CHPKs of animal herpesviruses, such as DEV, are comparatively scarce. In a previous study, our group isolated DEV, which was classified into alphaherpesvirinae, from the intestine of a sick duck and sequenced the genome. This analysis showed that DEV encodes a pUL13 showing 35~40% similarity with reported CHPKs in human herpesviruses, and 40~50% similarity with the CHPK of poultry herpesviruses.

There are few reports in DEV about pUL13. In order to study the function of DEV pUL13, it is necessary to know the location of pUL13 in the cells. The distribution of pUL13 in the nucleus and cytoplasm of DEV infected cells was observed by indirect immunofluorescence analysis. The fusion expression of DEV pUL13 and GFP showed that the green fluorescence was detected in the nucleus. Studies showed that the protein of more than 40 kDa had to rely on the active transport form [58, 59, 60]. DEV pUL13 homologous proteins, such as UL97 protein of HCMV, BGLF4 of EBV and U69 of human herpesvirus 6 (HHV-6) have been reported to be located in the nucleus [27, 61], and all of them contain nuclear localization signals to regulate their nuclear entry process [60-61]. There are few reports about the location of pUL13 in  $\alpha$ -herpesvirus, but early reports showed that pUL13 can be extracted from the nucleus of HSV-1 and HSV-2 infected cells [62]. The nuclear pore complex can allow soluble small molecules to import or export from the nuclear membrane. The transported substances include RNA, ribosome, protein, carbohydrate and signal molecules [63]. It is obvious that small molecules can pass through the nuclear pore complex through diffusion, while large molecules may enter and exit the nucleus with the help of nuclear pore proteins after being recognized by specific signal sequences [64-65]. Nuclear localization signal sequence is such a kind of amino acid sequence, which marks proteins and transports them into the nucleus. Therefore, proteins with nuclear localization signal can effectively enter the nucleus through the nuclear pore complex [66]. In conclusion, we speculate that DEV pUL13 also has nuclear localization signal.

Based on the analysis of biological information of DEV UL13, two basic amino acid enriched peptides were predicted, which were located at 4-7 aa and 90-96 aa respectively, which were potential nuclear localization signals. This result is consistent with the following results, further confirmed that NLS1 and NLS2 of pUL13 are functional nuclear localization signals, and the synergistic effect of NLS1 and NLS2 can enhance their nuclear localization ability. Study of DEV pUL13 homologous proteins, HCMV UL97 and HHV U69, indicate that they are classical importin  $\alpha$  /  $\beta$  protein dependent pathways [58, 60]. It is reported that ivermectin can block the interaction between importin  $\alpha$  and importin  $\beta$  to inhibit the nuclear import dependent on the classical NLS. However, ivermectin is a specific inhibitor of importin  $\alpha$ /beta-mediated nuclear import able to inhibit replication of HIV-1 and dengue virus. Ivermectin can only selectively identify importin  $\alpha$  or importin  $\beta$  nuclear import containing NLSs, for other nuclear import pathways have no inhibition effect [67]. The prediction results of DEV pUL13 showed that the two nuclear localization signals NLS1 and NLS2 were classical 4 and 7 type nuclear localization signals. In order to explore whether the entry of DEV pUL13 into the nucleus is also a classical import  $\alpha$  /  $\beta$  protein dependent nuclear import pathway, we treated the cells with the recombinant plasmids of UL13-GFP and NLS1 & NLS2-GFP by ivermectin, and compared the difference of fluorescence distribution between the treated group and the untreated group. The results showed that the distribution of fluorescence in the nucleus of the transfected cells treated with ivermectin was less than that of the untreated cells, and the difference between the treated and untreated cells was very obvious. Ivermectin effectively inhibited the nuclear import of DEV pUL13 and NLS1 &

NLS2-GFP protein, which indicated that the nuclear localization signals of DEV pUL13 regulated nuclear import by forming complex with importin  $\alpha$  /  $\beta$ .

The cell biological characteristics of the successfully constructed NLS deletion and rescued DEV CHV BAC UL13 -  $\Delta$  NLS/ $\Delta$  NLSR mutant were analysed. Compared with the parent virus, it was found that there was no significant difference in size of the plaque and the growth and replication ability of UL13 -  $\Delta$  NLS recombinant virus. The results showed that pUL13 NLSs had little effect on virus replication. Among the members of  $\beta$  - herpesvirus subfamily and  $\gamma$  - herpesvirus subfamily, UL13 homologues have been reported to affect virus replication, for example, HCMV UL97 protein kinase affects virus replication by phosphorylating virus DNA polymerase extension factor UL44 [68]. EBV BGLF4 affects virus growth and replication by phosphorylating virus DNA elongation factor BMRF1 [69]. It has been reported that HSV-1 UL13 can promote the expression of a series of viral genes, including ICP22 and some late genes [70], but there is no further report about the effect of UL13 protein on viral replication in the members of  $\alpha$ -herpesvirus subfamily. This may be related to the existence of another conserved protein kinase, US3 protein kinase, in the subfamily of alpha herpesvirus. It is reported that US3 protein kinase has an important effect on the growth and replication of virus [71]. We also tested the kinase activity of UL13 -  $\Delta$  NLS protein in vivo, and found that the DEV UL13 protein without nuclear localization signal can still phosphorylate US3 protein, we speculate that the loss of nuclear localization signal has no significant effect on the activity of UL13 protein kinase, but the biological function of DEV UL13 protein in the nucleus needs further study.

## Conclusions

In our study, we identified that the nuclear import of DEV UL13 protein is directed by amino acids 4 to 7 and 90 to 96, and proved that this nuclear import occurs via the classical importin  $\alpha/\beta$  - dependent process. We also constructed a mutant virus with NLSs of UL13 deleted, and preliminarily explored characteristics of this mutant virus for further function study.

## Methods

### Cells and virus

The previously reported DEV CHv strain (Gen Bank No.JQ647509) was maintained in our lab[72-73] and slightly changes. Briefly, duck embryo fibroblasts (DEFs) were propagated in Minimal Essential Medium (MEM, Gibco-BRL, Grand Island, NY, USA) provided by our lab supplemented with 10% (v/v) foetal bovine serum (FBS, Gibco-BRL, Grand Island, NY, USA) and incubated at 37°C with 5% CO<sub>2</sub>.

### Analysis of sequence motifs within UL13

Putative nuclear localization signals (NLSs) within the UL13 coding sequence were identified using PSORT II Prediction (<http://psort.nibb.ac.jp/form2.html>) [74]. Sequence analysis using PSORT II predicted that UL13 has two potential NLSs in its arginine-rich regions, namely, RRRR at aa 4 to 7 and PGKRKTK at aa 90 to 96 (Figure S1).

### Construction of recombinant plasmids

The experimental operation was carried out as described previously [75-77]. Briefly, the full-length UL13 sequence was amplified from DEV chromosomal DNA using the primers F-UL13F and F-UL13R. UL13- $\Delta$ NLS1 was PCR amplified from DEV chromosomal DNA using the primers  $\Delta$ NLS1F and F-UL13R. UL13- $\Delta$ NLS2 was amplified by

overlapping PCR from DEV chromosomal DNA using the primers F-UL13F,  $\Delta$ NLS2R,  $\Delta$ NLS2F, and F-UL13R. UL13- $\Delta$ NLS1& $\Delta$ NLS2 was PCR amplified from pEGFP-N1-UL13- $\Delta$ NLS2 DNA using the primers  $\Delta$ NLS1F and F-UL13R (Tables 1). The PCR fragments were purified and digested with EcoRI and HindIII and ligated into the pEGFP-N1 plasmid digested with the corresponding restriction endonucleases. The ligation mixtures were introduced into CaCl<sub>2</sub>-competent E. coli DH5 $\alpha$  cells, and transformants were selected on LB plates containing 50  $\mu$ g/ml Kan. Clones were screened by PCR with the corresponding primers. The validity of the sequences was determined by sequencing. The GFP, NLS1-GFP, NLS2-GFP and NLS1&NLS2-GFP genes were amplified by PCR from pEGFP-N1 DNA using the primers GFPF and GFPR; NLS1F and GFPR; NLS2F and GFPR; and NLS1&NLS2F and GFPR, respectively (Table 1). These PCR fragments were purified and digested with EcoRI and HindIII. Then, the purified fragments were ligated into the pcDNA3.1(+) plasmid digested with the corresponding restriction endonucleases. Ligation mixtures were introduced into the CaCl<sub>2</sub>-competent E. coli DH5 $\alpha$  strain, and transformants were selected on LB plates containing Amp at 100  $\mu$ g/ml. Clones were screened by PCR with the corresponding primers. Sequencing was used for confirmation.

**Table 1.** Oligonucleotide primers used in this work

Oligonucleotide primer	Sequence <sup>a</sup> (5'-3')
T-UL13F	GGATCCCTGGTGGCTACGGAGAG
T-UL13R	AAGCTTCCAAGGGCGTATATGTC
F-UL13F	<i>ccc</i> AAGCTTATGGCTGGACGAAGACG
F-UL13R	<i>ccg</i> GAATTCTGTTATAAAATCCACAATAGAG
$\Delta$ NLS1F	<i>ccc</i> AAGCTTATGGCTGGAAGCCCTATTAGCGAAATG
$\Delta$ NLS2R	CATCTACTATCCTTTCTCTTTACTG
$\Delta$ NLS2F	GAAAGGATAGTAGATGGAGCCTGG
GFPF	<i>ccc</i> AAGCTTATGGTGGAGCAAGGGCG
GFPR	<i>ccg</i> GAATTCTGATTATGATCTAGAGTCG
NLS1F	<i>ccc</i> AAGCTTATGGCTGGACGAAGACGACGAAGCCCTATGGTGGAGCAAGGGCG
NLS2F	<i>ccc</i> AAGCTTATGAAGGATCCTGGCAAACGTAAGACAAAGAGTAGAATGGTGGAG CAAGGGCG
NLS1&NLS2F	<i>ccc</i> AAGCTTATGGCTGGACGAAGACGACGAATGAAGGATCCTGGCAAAC

<sup>a</sup>The sequences of restriction endonuclease sites are in *italics*, and lowercase letters denote protective bases.

## Immunofluorescence assay

The experimental operation was carried out as described previously and slightly change[78-82]. Briefly, DEF cells were fixed with 4% paraformaldehyde at 16h post-transfection, permeabilized with 0.1% Triton X-100 and blocked with bovine serum albumin (BSA) for 1h. The cells were incubated with the rabbit anti-UL13 antiserum (1:200 dilution) for 1h at 37°C and then with a goat anti-rabbit antibody conjugated to fluorescein isothiocyanate at a dilution of 1:200 (FITC, Zhongshan, Beijing, China) for 30 min. The nuclei were stained with DAPI. The cells were observed using a Nikon ECLIPSE 80i microscope.

## Extraction and analysis of cytoplasmic/nuclear proteins

The experimental operation was carried out as described previously [83]. Briefly, confluent monolayers of DEF cells were transfected with pEGFP-N1-UL13 or pEGFP-N1-UL13- $\Delta$ NLS1& $\Delta$ NLS2 plasmids (2.5 $\mu$ g/well) in 6-well plates for 16h and harvested after washing twice with PBS. The cells were pelleted by centrifugation at 3,000 rpm for 5 min and resuspended in 20  $\mu$ l cytosol extraction buffer (10  $\mu$ l 1 M HEPES (pH 7.5); 6  $\mu$ l 100% Triton X-100; 50  $\mu$ l 3

M NaCl; 2 µl 0.5 M EDTA; 50 µl 200µg/ml protease inhibitor; 882 µl ddH<sub>2</sub>O) and incubated for 5 min on ice. The suspension was separated into nuclear and cytoplasmic fractions by 4,000 rpm for 5 min. The nuclear fraction was resuspended in 15 µl nuclear extraction buffer (20 µl 1 M HEPES (pH 7.5); 250 µl 100% glycerol; 140 µl 3 M NaCl; 12 µl 100 mM MgCl<sub>2</sub>; 4 µl 0.5 M EDTA; 5 µl 1 M DTT; 50 µl 200µg/ml protease inhibitor; 527.1 µl ddH<sub>2</sub>O) and incubated for 30 min on ice, meanwhile, strongly mixed by vortexing six times for 30 s. The supernatant was collected by centrifugation for 30 min at 14,000 rpm at 4°C. The obtained cytoplasmic/nuclear proteins were subjected to western blotting according to the protocol described above. The anti-UL13 antibody, rabbit anti-β-actin antibody (APGBIO Ltd, Shanghai, China) and rabbit anti-Lamin A/C antibody (Signalway Antibody, Maryland, USA) were used as primary antibody, separately. Protein bands were visualized by using ECL Western blotting detection reagents (Bio-Rad, California, USA) according to the manufacturer's instructions.

### **Analysis of pharmaceutical inhibition of nucleus/cytoplasm transport**

The experimental operation was carried out as described previously [84-85]. Briefly, DEFs were cultured in MEM supplemented with 10% (v/v) FBS at 37°C with 5% CO<sub>2</sub>. Lipofectamine 2000 was used according to the manufacturer's instructions to transfect the pEGFP-N1-UL13 or pcDNA3.1(+)-NLS1&NLS2-GFP recombinant plasmid (2.5µg per well) into DEFs in 6-well cell culture plates. Where appropriate, cells were treated with ivermectin at a final concentration of 25 µM for 1 h before imaging [86-88]. Cells were imaged live at 16h after transfection using a Nikon ECLIPSE 80i microscope. To determine the nuclear/cytoplasmic fluorescence ratio, digitized images were analysed using the Image-Pro Plus software. Statistical analysis was performed using the GraphPad Prism 6.0 software.

### **Construction of Recombinant Viruses DEV CHv-UL13ΔNLS**

To create the DEV CHv-UL13ΔNLS virus, with both NLS1 and NLS2 of UL13 deleted, we need to create the UL13 and UL14 gene-deleted recombinant mutant, DEV CHv-ΔUL13&UL14 virus first according to the overlapping of UL13 gene and UL14 gene regions. The target segment (UL13 left arm-FRT-Kan-FRT-UL14 right arm) was PCR-amplified using the ΔUL13&UL14 F F/R primers (Table 2). Then, the infectious clone DEV CHv-ΔUL13&UL14-G was generated by employing a recombining system based on the genetic manipulation of the DEV CHv-G infectious clone[34-37]. Briefly, the pKD46 plasmid, which encodes the recombination genes *exo*, *beta*, and *gam* under the tight control of a *ParaB* promoter, was first introduced into *E. coli* DH10B containing the DEV CHv-G plasmid by electrophoretic transfer. In this system, the UL13&UL14 coding sequence was replaced by the target segments amplified from the pKD4 plasmid. Next, the pCP20 plasmid was transferred into the above cells, which contain DEV CHv-ΔUL13&UL14-G and kanamycin-resistant gene cassette. Removal of the kanamycin-resistant cassette was accomplished by incubation at 30°C for 8 h then at 42°C overnight. Then we generated the DEV CHv-UL13ΔNLS-G and the revertant, DEV CHv-UL13ΔNLS R-G based on the same method used above but with two different target segments. Target segment of DEV CHv-UL13ΔNLS-G, UL13ΔNLS-UL14-FRT-Kan-FRT-UL14 right arm, which was fusion PCR-amplified using the UL13-ΔNLS F1X/UL13-ΔNLS R1, UL13-ΔNLS F2/ΔUL13(K179M) R and FRT-Kan F/ R primers (Table 2) with the pEGFP-N1:: UL13-ΔNLS1&ΔNLS2 plasmids, the CHv genome and the pKD4 plasmid as template, respectively; target segment of DEV CHv-UL13ΔNLS R-G, UL13-UL14-FRT-Kan-FRT-UL14 right arm, using the UL13-ΔNLS F1/ΔUL13(K179M) R and FRT-Kan F/ R primers (Table 2) with the CHv genome and the pKD4 plasmid as template, respectively. The DEV CHv-UL13ΔNLS-G and DEV CHv-UL13ΔNLS R-G infectious clones, were identified by sequencing and RFLP analysis. Finally, the DEV CHv-UL13ΔNLS and DEV CHv-UL13ΔNLS R recombinant viruses were rescued; freshly prepared DEV CHv-UL13ΔNLS -G and DEV CHv-UL13ΔNLS R-G plasmids were transfected into DEFs for one to 10 d, and the cells were examined by fluorescence microscopy

until green fluorescence protein seemed sufficiently expressed, at which point, they were harvested after freeze-thawing 3 times. After amplifying the DEV CHv-UL13ΔNLS and DEV CHv-UL13ΔNLS R viruses, viral PCR identification and sequencing of the target region were performed.

**Table 2.** Primers used for Red recombination to construct the CHv-BAC-UL13-Δ

NLS

Oligonucleotide primer	Sequence (5'-3')
pKD46 F	AAAGCCGCAGAGCAGAAGGTGG
pKD46 R	GGTAAACGGGCATTTCAAGG
ΔUL13&UL14 F	ATATGATTTGTTTTTTCCTACTCTATTGAATAGTGCGCACTCTCGCTAACGTGTAGGCTGGAGCTGCTTC
ΔUL13&UL14 R	ACGTTTGCAGTGATGTACTGGCGATGAGCTACCATCTATATCCCCACTCATGGTAGCATATGAATATCCTCCTTAG
UL13-ΔNLS F1	CTTCACATAATACGCCACTGATC
UL13-ΔNLS F1X	GCGCAAAGGCTGCAATACG
UL13-ΔNLS R1	CCGATAGGATTCATTTGCTAATAGGGCTTCCAGCCATTTCGTTACCAGATAGTC
UL13-ΔNLS F2	GACTATCTGGTAACGAATGGCTGGAAGCCCTATTAGCGAAATG AATCCTATCGG
ΔUL13(K179M) R	TTAGTTATAAATCCACAATAGAG
FRT-Kan F	AGAAGCGCCGCTCCTCTATTGTGGATTATAACTAAGTGTAGGCTGGAGCTGCTTC
FRT-Kan R	ACGTTTGCAGTGATGTACTGGCGATGAGCTACCATCTATATCCCCACTCATGGTAGCATATGAATATCCTCCTTAG

## Plaque Assay

The experimental operation was carried out as described previously [89-90]. Briefly, DEFs were incubated with DEV CHv, DEV CHv-UL13ΔNLS, or DEV CHv-UL13ΔNLS R at 37°C for 2 hours. The plates were then overlaid with an equal-parts mixture of 2 × MEM and 0.5% methylcellulose (9004-67-5, J & K SCIENTIFIC LTD., Beijing, China) after discarding unabsorbed particles. After incubation at 37°C for 6 d, the cells were fixed with 4% paraformaldehyde and stained with 0.05% crystal violet (C3886, Haoran Bio, Beijing, China). Plaque areas were then measured by Image Pro Plus software, with 50 plaques chosen at random for each virus.

## Growth Curve Assay

The experimental operation was carried out as described previously and slightly changes [91]. Briefly, duck embryo fibroblasts cells were infected with DEV CHv, DEV CHv-UL13ΔNLS, or DEV CHv-UL13ΔNLS R at 200 TCID<sub>50</sub>. The cells were maintained in MEM supplemented with 2% FBS, and samples of the cells and supernatants were separately harvested at 6, 12, 24, 48, 72, and 96 h for the growth curve assay after being freeze-thawed 3 times. The growth curve was recorded via measuring the TCID<sub>50</sub>, which was calculated with the Reed Muench method, and the samples at different time points and triplicate experiments were performed.

## List Of Abbreviations

Abbreviation	Full name
DEV	<i>Duck enteritis virus</i>
CHPK	Conserved herpesvirus protein kinase
NLS	Nuclear localization signals
HSV	Herpes simplex virus
HCMV	Human cytomegalovirus
KSHV	Kaposi's sarcoma-associate herpesvirus
DEF	Duck embryo fibroblasts
EBV	Epstein-barr virus
IRF3	Interferon regulatory factor 3
SOCS-3	Suppressor of cytokine signalling 3

## Declarations

### Acknowledgments

The authors thank AC and MW for review and revision and long-term spurs. We also thank AC and MW for their motivation in the experimental process of this paper.

### Author contributions

LY and XH conceived, designed and performed most experiments; analysed the data; and drafted the manuscript. AC and MW conceived and supervised the study. RJ,QY, YW, SC, ML, DZ, XO, XW, SM, DS, SZ, XZ, JH, QG, YL, YY, LZ, BT, LP, RU and XC interpreted the data. All authors read and approved the final manuscript for publication.

### Funding

This work was supported by the National Key Research and Development Program of China (2017YFD0500800), the China Agricultural Research System (CARS-42-17), the Sichuan Veterinary Medicine and Drug Innovation Group of China Agricultural Research System (CARS-SVDIP) and Integration and Demonstration of Key Technologies for Goose Industrial Chain in Sichuan Province (2018NZ0005). The funders supervised of the study and did not have any role in the collection, analysis, and interpretation of data or in writing the manuscript.

### Availability of data and materials

The datasets used and/or analyzed during the current study are available from the corresponding author on reasonable request.

### Ethics approval and consent to participate

The study was approved by the Committee of Experiment Operational Guidelines and Animal Welfare of Sichuan Agricultural University. Preparing fibroblast cells was conducted in accordance with approved guidelines.

### Consent for publication

Not applicable.

### Competing interest

The authors have no competing interests to declare.

## References

1. Qi X, Cheng A, Wang M, Zhu D, Jia R. The Pathogenesis of Duck Virus Enteritis in Experimentally Infected Ducks: A Quantitative Time-Course Study Using TaqMan Polymerase Chain Reaction. *Avian Pathology*. 2008; 37, 307-10.
2. Yuan G, Cheng A, Wang M, Liu F, Han X, Liao Y. et al. Preliminary study on duck enteritis virus-induced lymphocyte apoptosis in vivo. *Avian Dis*. 2007; 51:546–9.
3. Qi X, Yang X, Cheng A, Wang M, Zhu D, Jia R. et al. Intestinal mucosal immune response against virulent duck enteritis virus infection in ducklings. *Res Vet Sci*. 2009; 87:218–25.
4. Liu T, Cheng A, Wang M, Jia R, Yang Q, Wu Y. et al. RNA-seq comparative analysis of Peking ducks spleen gene expression 24 h post-infected with duck plague virulent or attenuated virus. *Vet Res*. 2017; 48:47.
5. King A, Adams M, Lefkowitz EJ. *Virus taxonomy: ninth report of the International Committee on Taxonomy of Viruses*. Elsevier. 2012.
6. Cheng A. *Duck plague*. Beijing, China agriculture press. 2015.
7. Wu Y, Cheng A, Wang M, Yang Q, Zhu D, Jia R. et al. Complete Genomic Sequence of Chinese Virulent Duck Enteritis Virus. *J Virol*. 2012; 86: 5965-5965.
8. Hu X, Wang M, Chen S, Jia R, Zhu D, Liu M. et al. The duck enteritis virus early protein, UL13, found in both nucleus and cytoplasm, influences viral replication in cell culture. *Poult Sci*. 2017; 96(8):2899-2907.
9. Lee CP, Huang Y, Lin S, Chang Y, Chang Y, Takada, K. et al. Epstein-Barr virus BGLF4 kinase induces disassembly of the nuclear lamina to facilitate virion production. *J virol*. 2008; 82(23): 11913-11926.
10. Marschall M, Marzi A, aus dem Siepen P, Jochmann R, Kalmer M, Auerochs S. et al. Cellular p32 recruits cytomegalovirus kinase pUL97 to redistribute the nuclear lamina. *J Biol Chem*. 2005; 280(39): 33357-33367.
11. Krosky P, Baek MC, Coen DM. The human cytomegalovirus UL97 protein kinase, an antiviral drug target, is required at the stage of nuclear egress. *J virol*. 2003; 77(2): 905-914.
12. Prichard MN, Britt WJ, Daily SL, Hartline CB, Kern ER. Human cytomegalovirus UL97 kinase is required for the normal intranuclear distribution of pp65 and virion morphogenesis. *J virol*. 2005, 79(24): 15494-15502.
13. Cano-Monreal GL, Wylie KM, Cao F, Tavis JE, Morrison LA. Herpes simplex virus 2 UL13 protein kinase disrupts nuclear lamins. *Virology*. 2009; 392(1):137-147.
14. Akihisa K, Yamamoto M, Ohno T, Tanaka M, Sata T, Nishiyama Y. et al. Herpes simplex virus 1-encoded protein kinase UL13 phosphorylates viral Us3 protein kinase and regulates nuclear localization of viral envelopment factors UL34 and UL31. *J Virol*. 2006; 80(3): 1476-1486.
15. Marschall M, Freitag M, Suchy P, Romaker D, Kupfer R, Hanke M. et al. The protein kinase pUL97 of human cytomegalovirus interacts with and phosphorylates the DNA polymerase processivity factor pUL44. *Virology*. 2003; 311(1): 60-71.
16. Yang P, Chang S; Tsai C, Chao Y, Chen M. Effect of phosphorylation on the transactivation activity of Epstein-Barr virus BMRF1, a major target of the viral BGLF4 kinase. *J Gen Virol*. 2008; 89(4): 884-895.
17. Tarakanova VL, Leung-Pineda V, Hwang S, Yang C, Matatall K, Basson M. et al.  $\gamma$ -herpesvirus kinase actively initiates a DNA damage response by inducing phosphorylation of H2AX to foster viral replication. *Cell host microbe*. 2007; 1(4): 275-286.
18. Baek MC, Krosky PM, Pearson A, Coen DM. Phosphorylation of the RNA polymerase II carboxyl-terminal domain in human cytomegalovirus-infected cells and in vitro by the viral UL97 protein kinase. *Virology*. 2004;

324(1):184-193.

19. Tamrakar S, Kapasi AJ, Spector DH. Human cytomegalovirus infection induces specific hyperphosphorylation of the carboxyl-terminal domain of the large subunit of RNA polymerase II that is associated with changes in the abundance, activity, and localization of cdk9 and cdk7. *J virol.* 2005; 79(24): 15477-15493.
20. Paladino P, Marcon E, Greenblatt J, Frappier L. Identification of herpesvirus proteins that contribute to G1/S arrest. *J virol.* 2014; 88(8):4480-4492.
21. Chang YH, Lee CP, Su M, Wang J, Chen J, Lin S. et al. Epstein-Barr virus BGLF4 kinase retards cellular S-phase progression and induces chromosomal abnormality. *PloS one.* 2012; 7(6): e39217.
22. Hwang S, Kim KS, Flano E, Wu T, Tong LM, Park AN. et al. Conserved herpesviral kinase promotes viral persistence by inhibiting the IRF-3-mediated type I interferon response. *Cell host microbe.* 2009; 5(2):166-178.
23. Wang J, Doong SL, Teng SC, Lee CP, Tsai CH, Chen MR. Epstein-Barr virus BGLF4 kinase suppresses the interferon regulatory factor 3 signaling pathway. *J virol.* 2009; 83(4): 1856-1869.
24. Yokota S, Yokosawa N, Okabayashi T, Suzutani T, Miura S, Jimbow K. et al. Induction of suppressor of cytokine signaling-3 by herpes simplex virus type 1 contributes to inhibition of the interferon signaling pathway. *J virol.* 2004; 78(12): 6282-6286.
25. Littler E, Stuart AD, Chee MS. Human cytomegalovirus UL97 open reading frame encodes a protein that phosphorylates the antiviral nucleoside analogue ganciclovir. *Nature.*1992; 358: 160-162.
26. Michel D, Schaarschmidt P, Wunderlich K, Heuschmid M, Simoncini L, Mühlberger D. et al. Functional regions of the human cytomegalovirus protein pUL97 involved in nuclear localization and phosphorylation of ganciclovir and pUL97 itself. *J Gen virol.* 1998; 79(9): 2105-2112.
27. Leen D, Bolle DM, Mertens T, Manichanh C, Agut H, Clercq ED. et al. Role of the Human Herpesvirus 6 U69-Encoded Kinase in the Phosphorylation of Ganciclovir. *Mol Pharmacol.* 2002; 62(3):714-721.
28. Cannon JS, Hamzeh F, Moore S, Nicholas J, Ambinder RF. Human herpesvirus 8-encoded thymidine kinase and phosphotransferase homologues confer sensitivity to ganciclovir. *J Virol.* 1999; 73(6):4786-4793.
29. Meng Q, Hagemeyer SR, Fingerroth JD, Gershburg E, Pagano JS, Kenney SC. The Epstein-Barr virus (EBV)-encoded protein kinase, EBV-PK, but not the thymidine kinase (EBV-TK), is required for ganciclovir and acyclovir inhibition of lytic viral production. *J virol.* 2010; 84(9):4534-4542.
30. Zhou X, Wang M, Cheng A, Yang Q, Wu Y, Jia R. et al. Development a simple and rapid immunochromatographic strip test for detecting antibody of duck plague virus based on gI protein. *J Virol Method.* 2020; 277: 113803, doi: org/10.1016/j.jviromet.2019.113803.
31. Yang L, Wang M, Zeng C, Shi Y, Cheng A, Liu M. et al. Duck enteritis virus UL21 is a late gene and encodes a protein that interacts with pUL16. *BMC Vet Res.* 2020;16:8.
32. Zhao C, He T, Xu Y, Wang M, Cheng A, Zhao X. et al. Molecular characterization and antiapoptotic function analysis of the duck plague virus Us5 gene. *Sci Rep.* 2019; 9:4851.
33. Ma Y, Zeng Q, Wang M, Cheng A, Jia R, Yang Q. et al. US10 Protein Is Crucial but not Indispensable for Duck Enteritis Virus Infection in Vitro. *Sci Rep.* 2018; 8 (1), 16510.
34. Feng D, Cui M, Jia R, Liu S, Wang M, Yang Q. et al. Co-localization of and Interaction between Duck Enteritis Virus Glycoprotein H and L. *BMC Vet Res.* 2018; 14 (1), 255.
35. You Y, Liu T, Wang M, Cheng A, Jia R, Yang Q. et al. Duck plague virus Glycoprotein J is functional but slightly impaired in viral replication and cell-to-cell spread. *Sci Rep.* 2018; 8(1):4069.

36. Yang L, Wang M, Cheng A, Yang Q, Wu Y, Jia R. et al. Innate immune evasion of alphaherpesvirus tegument proteins. *Front immunol.* 2019; 10:2196.
37. Jing Y, Wu Y, Sun K, Wang M, Cheng A, Chen S. et al. Role of duck plague virus glycoprotein C in viral adsorption: Absence of specific interactions with cell surface heparan sulfate. *Journal of Integrative Agriculture.* 2017; 16(5): 1145-1152.
38. Liu C, Cheng A, Wang M, Chen S, Jia R, Zhu D. et al. Regulation of viral gene expression by duck enteritis virus UL54. *Sci Rep.* 2017; 7(1): 1076.
39. Wu Y, Li Y, Wang M, Sun K, Jia R, Chen S. et al. Preliminary study of the UL55 gene based on infectious Chinese virulent duck enteritis virus bacterial artificial chromosome clone. *Virol J.* 2017; 14(1): 78.
40. Gao J, Cheng A, Wang M, Jia R, Zhu D, Chen S. et al. Identification and characterization of the duck enteritis virus (DEV) US2 gene. *Genets Mol Res.* 2015; 29; 14 (4): 13779-13790.
41. He T, Wang M, Cao X, Cheng A, Wu Y, Yang Q. et al. Molecular characterization of duck enteritis virus UL41 protein. *Virol J.* 2018; 15:12.
42. Zhang D, Lai M, Wu Y, Yang Q, Liu M, Zhu D. et al. Molecular characterization of the duck enteritis virus US10 protein. *Virol J.* 2017; 14:183.
43. Liu C, Cheng A, Wang M, Chen S, Jia R, Zhu D. et al. Duck enteritis virus UL54 is an IE protein primarily located in the nucleus. *Virol J.* 2015;12: 198.
44. Lin M, Jia R, Wang M, Gao X, Zhu D, Chen S. et al. Molecular Characterization of Duck Enteritis Virus CHV Strain UL49.5 protein and its Colocalization with Glycoprotein M. *J Vet Sci.* 2014; 15(3): 389-39.
45. Sun K, Cheng A, Wang M. Bioinformatic analysis and characteristics of glycoprotein C encoded by the newly identified UL44 gene of duck plague virus. *Genet Mol Res.* 2014; 13(2): 4505 – 4515.
46. Wang M, Lin D, Zhang S, Zhu D, Jia R, Chen X. et al. Prokaryotic expression of the truncated duck enteritis virus UL27 gene and characteristics of UL27 gene and its truncated product. *Acta virol.* 2012; 56: 323-28.
47. He Q, Cheng A, Wang M, Xiang J, Zhu D, Zhou Y. et al. Replication kinetics of duck enteritis virus UL16 gene in vitro. *Virol J.* 2012; 9:281.
48. Xiang J, Zhang S, Cheng A, Wang M, Chang H, Shen C. et al. Expression and characterization of recombinant VP19c protein and N-terminal from Duck Enteritis Virus. *Virol J.* 2011; 8: 82.
49. Zhang S, Xiang J, Cheng A, Wang M, Wu Y, Yang X. et al. Characterization of duck enteritis virus UL53 gene and glycoprotein K. *Virol J.* 2011; 8:235
50. Li L, Cheng A, Wang M, Zhang S, Xiang J, Yang X. et al. Expression and Characterization of Duck Enteritis Virus gl Gene. *Virol J.* 2011; 8:241.
51. He Q, Yang Q, Cheng A, Wang M, Xiang J, Zhu D. et al. Expression and characterization of UL16 gene from duck enteritis virus. *Virol J.* 2011; 8:413.
52. Xie W, Cheng A, Wang M, Chang H, Zhu D, Luo Q. Molecular cloning and characterization of the UL31 gene from Duck enteritis virus. *Mol Bio Rep.* 2010;37 (3):1495-1503.
53. Cai M, Cheng A, Wang M, Chen W, Zhang X, Zheng S. et al. Characterization of the duck plague virus UL35 gene. *Intervirolgy.* 2010; 53:408-416
54. Lian B, Chao X, Cheng A, Wang M, Zhu D, Luo Q. et al. Identification and characterization of duck plague virus glycoprotein C gene and gene products. *Virol J.* 2010; 7:349

55. Gao X, Jia R, Wang M, Yang Q, Chen S, Liu M. et al. Duck enteritis virus (DEV) UL54 protein, a novel partner, interacts with DEV UL24 protein. *Virology*. 2017;14(1): 166.
56. Li Y, Wu Y, Wang M, Ma Y, Jia R, Chen S. et al. Duplicate US1 genes of duck enteritis virus encode a non-essential immediate early protein localized to the nucleus. *Front Cell Infect Microbiol*. 2020; 9, 463.
57. Thary J, Céline Van den B, Herman WF. Viral serine/threonine protein kinases. *J virol*. 2011; 85(3): 1158-1173.
58. Yuji Isegawa YM, Yasuda Y, Semi K, Tsujimura K, Fukunaga R, Ohshima A. et al. Characterization of the human herpesvirus 6 U69 gene product and identification of its nuclear localization signal. *J virol*. 2008; 82(2): 710-718.
59. Gershburg S, Murphy L, Marschall M, Gershburg E. Key motifs in EBV (Epstein-Barr virus)-encoded protein kinase for phosphorylation activity and nuclear localization. *Biochemical J*. 2010; 431(2): 227-235.
60. Rike Weibel JM, Auerochs S, Schregel V, Held C, No<sup>o</sup> Bauer K, RazzaziFazeli E. et al. Two isoforms of the protein kinase pUL97 of human cytomegalovirus are differentially regulated in their nuclear translocation. *J Gen Virol*. 2011; 92(92): 638-649.
61. Gershburg E, Marschall M, Hong K, Pagano JS. Expression and localization of the Epstein-Barr virus-encoded protein kinase. *J Virol*. 2004; 78(22): 12140-12146.62. Daikoku T, Shibata S, Goshima F, Oshima S, Tsurumi T, Yamada H. et al. Purification and Characterization of the Protein Kinase Encoded by the UL13 Gene of Herpes Simplex Virus Type 2. *Enzyme & Microbial Technology*. 1997; 235(1): 82-93.
62. Fernandez -Martinez J, Phillips J, Sekedat MD , Diaz-Avalos R, Velazquez-Muriel J, Franke JD. et al. Structure -function mapping of a heptameric module in the nuclear pore complex. *J Cell Biol*. 2012;196(4):419-434.
63. Miller M, Park MK, Hanover JA. Nuclear pore complex: structure,function, and regulation. *Physiological reviews*. 1991;71 (3):909-949.
64. Schmidt-Zachmann MS, Nigg EA. Protein localization to the nucleolus:a search for targeting gdomains in nucleolin. *J Cell Sci*.1993;105 (3):799-806.
65. Ohshima K, Takeda S, Hirose M, Akiyama Y, Iguchi K, Hoshino M. et al. Structure -function relationship of the nuclear localization signal sequence of parathyroid hormone -related protein. *Biomed Res*. 2012; 33(3):191-199.
66. Wagstaff KM, Sivakumaran H, Heaton SM, Harrich D, Jans DA. Ivermectin is a specific inhibitor of importin alpha/beta-mediated nuclear import able to inhibit replication of HIV-1 and dengue virus. *Biochem J*. 2012; 443(3):851-856.
67. Krosky PM, Moon-Chang B, Coen DM. The Human Cytomegalovirus UL97 Protein Kinase, an Antiviral Drug Target, Is Required at the Stage of Nuclear Egress. *J Virol*. 2003; 77(2): 905-914.
68. Chen M, Chang S, Huang H, Chen J. A protein kinase activity associated with Epstein-Barr virus BGLF4 phosphorylates the viral early antigen EA-D in vitro. *J Virol*. 2000; 74(7):3093-3104.
69. Purves F, Ogle W, Roizman B. Processing of the herpes simplex virus regulatory protein  $\alpha$ 22 mediated by the UL13 protein kinase determines the accumulation of a subset of  $\alpha$  and  $\gamma$  mRNAs and proteins in infected cells. *Proc Natl Acad Sci U S A*. 1993; 90(14): 6701-6705.
70. Reynolds AE, Wills EG, Roller RJ, Ryckman BJ, Baines JD. Ultrastructural localization of the herpes simplex virus type 1 UL31, UL34, and US3 proteins suggests specific roles in primary envelopment and egress of nucleocapsids. *J Virol*. 2002; 76(17):8939-8952.
71. Zhao L, Cheng A, Wang M, Yuan G, Cai M. Characterization of codon usage bias in the dUTPase gene of duck enteritis virus. *Progress in Natural Science*. 2008; 18(8):1069-1076.

72. Chang H, Cheng A, Wang M, Guo Y, Xie W, Luo Q. Complete nucleotide sequence of the Duck plague virus gE gene. *Arc Virol.* 2009; 154(1): 163-165.
73. Nakai, K.; Horton, P. PSORT: a program for detecting sorting signals in proteins and predicting their subcellular localization. *Trends in Biochemical Sciences.* 1999, 24(1):34-36.
74. Jia R, Cheng A, Wang M, Qi X, Zhu D, Ge H. et al. Development and evaluation of an antigen-capture ELISA for detection of the UL24 antigen of the duck enteritis virus, based on a polyclonal antibody against the UL24 expression protein. *J Virol Methods.* 2009; 161: 38–43.
75. Xie W, Cheng A, Wang M, Chang H, Zhu D, Luo Q. et al. Expression and characterization of the UL31 protein from duck enteritis virus. *Virol J.* 2009; 6:19.
76. Shen C, Guo Y, Cheng A, Wang M, Zhou Y, Lin D. et al. Characterization of subcellular localization of duck enteritis virus UL51 protein. *Virol J.* 2009; 6:92.
77. Jia R, Wang M, Cheng A, Zhu D, Ge H, Xin H. et al. Cloning, expression, purification and characterization of UL24 protein of Partial duck enteritis virus. *Intervirolgy.* 2009; 52:326-334.
78. Xin H, Cheng A, Wang M, Jia R, Shen C, Chang H. Identification and characterization of a duck enteritis virus US3-like gene. *Avian Dis.* 2009; 53(3): 363-370.
79. Zhang S, Xiang J, Cheng A, Wang M, Li X, Li L. et al. Production, purification and characterization of polyclonal antibody against the truncated gK of the duck enteritis virus. *Virol J.* 2010; 7:241.
80. Chang, H.; Cheng, A.C.; Wang, M.S.; Jia, R.Y.; Zhu, D.K.; Luo, Q.H.; Chen, Z.L.; Zhou, Y.; Liu, F.; Chen, X.Y. Immunofluorescence Analysis of Duck plague virus gE protein on DPV-infected ducks. *Virol J.* 2011, 8:19.
81. Zhang S, Cheng A, Wang M. Characteristics and functional roles of glycoprotein K of herpesviruses. *Reviews in Medical Microbiology.* 2011; 22(4):90–95.
82. Guo Y, Cheng A, Wang M, Zhou Y. Purification of anatisid herpesvirus 1 particles by tangential-flow ultrafiltration and sucrose gradient ultracentrifugation. *J Virol Methods.* 2009; 161(1):1-6.
83. Chang H, Cheng A, Wang M, Zhu D, Jia R, Liu F. et al. Cloning, Expression and Characterization of gE protein of Duck plague virus. *Virol J.* 2010; 7:120.
84. Shen A, Ma G, Cheng A, Wang M, Luo D, Lu L. et al. Transcription phase, protein characteristics of DEV UL45 and prokaryotic expression, antibody preparation of the UL45 des-transmembrane domain. *Virol J.* 2010; 7:232
85. Wagstaff KM, Sivakumaran H, Heaton SM, Harrich D, Jans DA. Ivermectin is a specific inhibitor of importin alpha/beta-mediated nuclear import able to inhibit replication of HIV-1 and dengue virus. *Biochem J.* 2012; 443(3):851-856.
86. Nishi K, Yoshida M, Fujiwara D, Nishikawa M, Horinouchi S, Beppu T. Leptomycin B targets a regulatory cascade of crm1, a fission yeast nuclear protein, involved in control of higher order chromosome structure and gene expression. *J Bio Chem.* 1994; 269(9):6320-6324.
87. Kudo N, Wolff B, Sekimoto T, Schreiner EP, Yoneda Y, Yanagida M. et al. Leptomycin B inhibition of signal-mediated nuclear export by direct binding to CRM1. *Exp Cell Res.* 1998; 242(2):540-547.
88. Guo Y, Shen C, Cheng A, Wang M, Chen S, Zhang N. et al. Anatisid herpesvirus 1 virulent strain induces syncytium and apoptosis in duck embryo fibroblast cultures. *Vet Microbiol.* 2009;138:258-265.
89. Yuan G, Cheng A, Wang M, Han X, Zhou Y, Liu F. Preliminary Study on Duck Enteritis Virus-Induced Lymphocyte Apoptosis In Vivo. *Avian dis.* 2007; 51(2):546–549.

90. Liu C, Cheng A, Wang M, Chen S, Jia R, Zhu D. et al. Characterization of nucleocytoplasmic shuttling and intracellular localization signals in Duck Enteritis Virus UL54. *Biochimie*. 2016;127: 86–94.

## Additional Files

Additional file 1. **Figure S1**. Online prediction of UL13 nuclear positioning signal through PSORT II. UL13 has two nuclear positioning signals.

## Figures

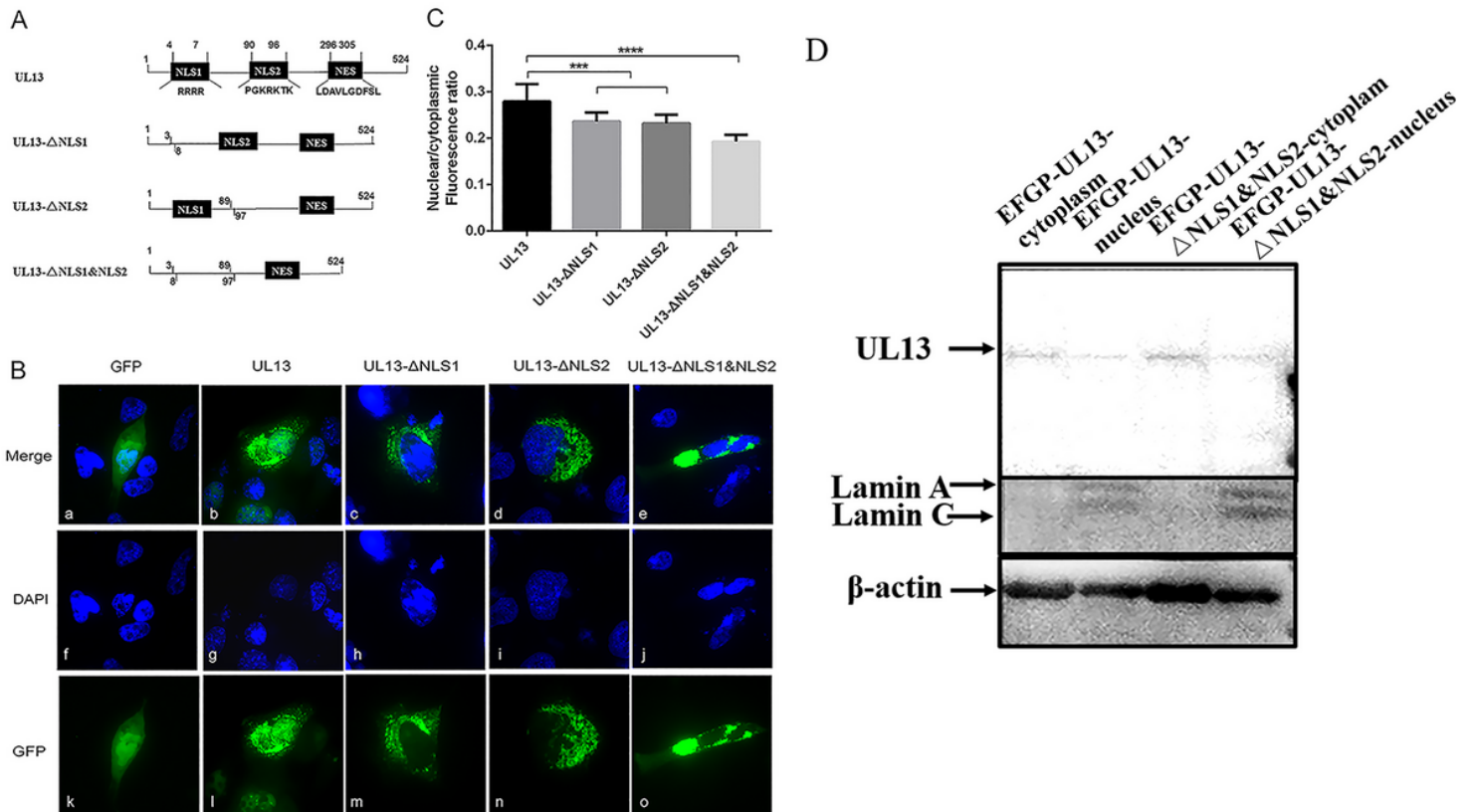


**Figure 1**

Localization of the UL13 and UL13-ΔNLS proteins in transfected DEFs. (A) Sketch map of the construction of UL13 with NLS deletion recombinant plasmids. (B) Verification of UL13/UL13-ΔNLS fusion protein localization via IFA. Plasmids of pEGFP-N1-UL13/UL13-ΔNLS were transfected into DEF cells. At 16h post transfection, the cells were fixed, permeabilized and incubated with rabbit anti-UL13 antiserum. Nuclei were stained with DAPI (blue). The expression and distribution of GFP protein (green) was monitored by fluorescence microscopy. Images were recorded in separate channels using a ×40 objective and merged in SPOT software. (C) The nuclear/cytoplasmic fluorescence ratio analysis. The ratio of nuclear and cytoplasmic distribution of fluorescence in the recombinant plasmid transfection group was calculated by Image Pro Plus. 50 cells in each group was analyzed. The ratio of nuclear and cytoplasmic fluorescence in the pEGFP-UL13-ΔNLS1, pEGFP-UL13-ΔNLS2 and pEGFP-UL13-ΔNLS1 & ΔNLS2 recombinant plasmid transfection group was analyzed by GraphPad prism 6.0 software. \*:  $P < 0.05$  \*\*:  $P < 0.01$ . (D) The nuclear/cytoplasmic distribution of the pUL13-NLS1&NLS2 deletion plasmids through western blot.

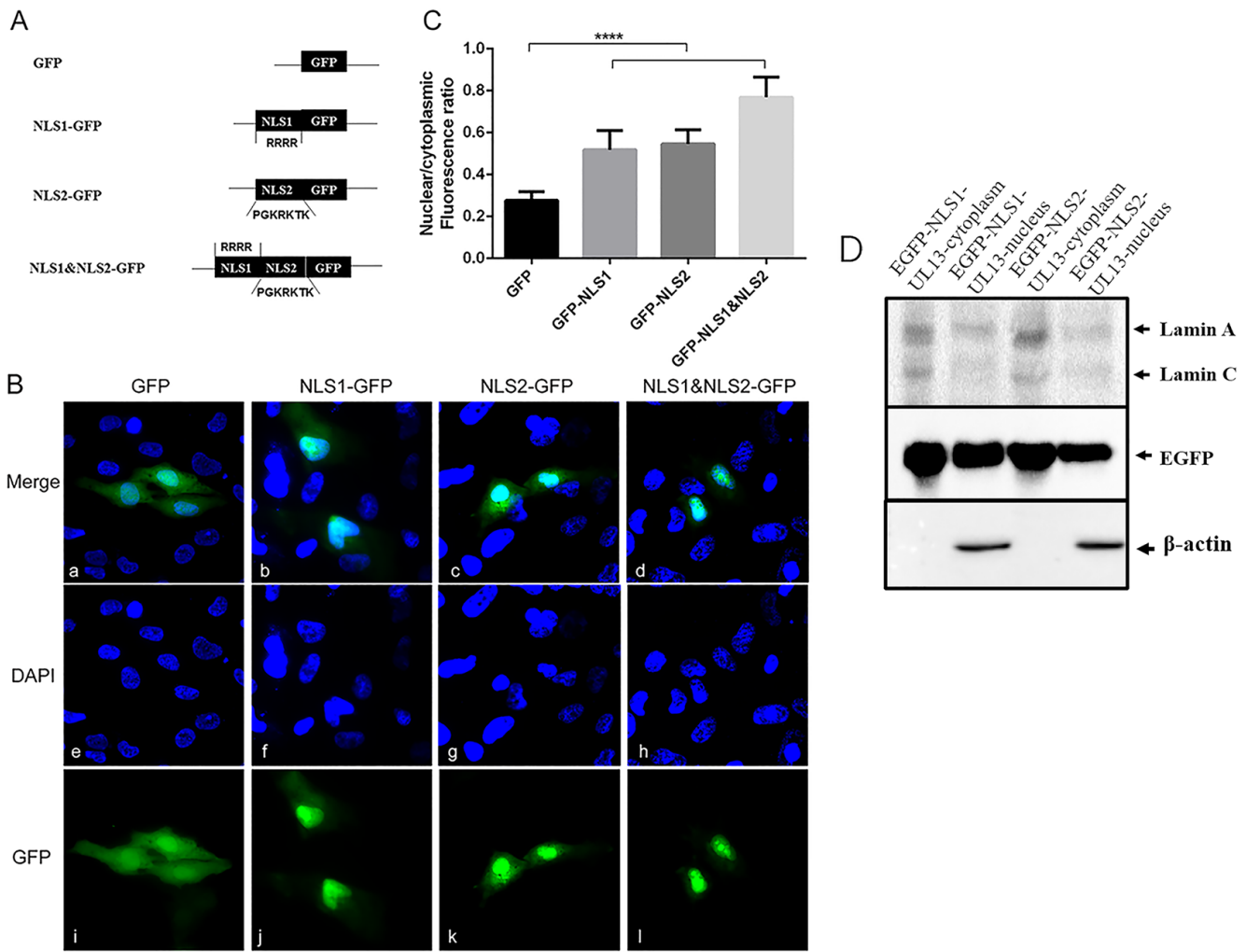


**Figure 2**

Construction of NLSs-GFP recombinant plasmids and localization analysis of the fusion proteins. (A) Sketch map of the construction of UL13 with NLS fusion protein recombinant plasmids. (B) Localization of the NLS-GFP fusion proteins in transfected DEFs. NLS-GFP recombinants were transfected into DEF cells, which were then fixed at 16h post transfection. Images of the GFP reporter (green) and nuclei stained with DAPI (blue) were recorded in separate channels using a  $\times 40$  objective and merged in SPOT software. (C) Comparison of the nuclear and cytoplasmic fluorescence ratio between GFP and NLS-GFP fusion protein. Mean nuclear and cytoplasmic fluorescence ratio was quantified using Image-Pro Plus software; analysis of the differences in the nuclear and cytoplasmic fluorescence ratios between GFP and the NLS1-GFP/NLS2-GFP/ NLS1&NLS2-GFP proteins was performed using ANOVA with GraphPad Prism 6.0 software. N=50 for each group. (D) The nuclear/cytoplasmic distribution of pUL13 NLS1 and NLS2 through western blot.

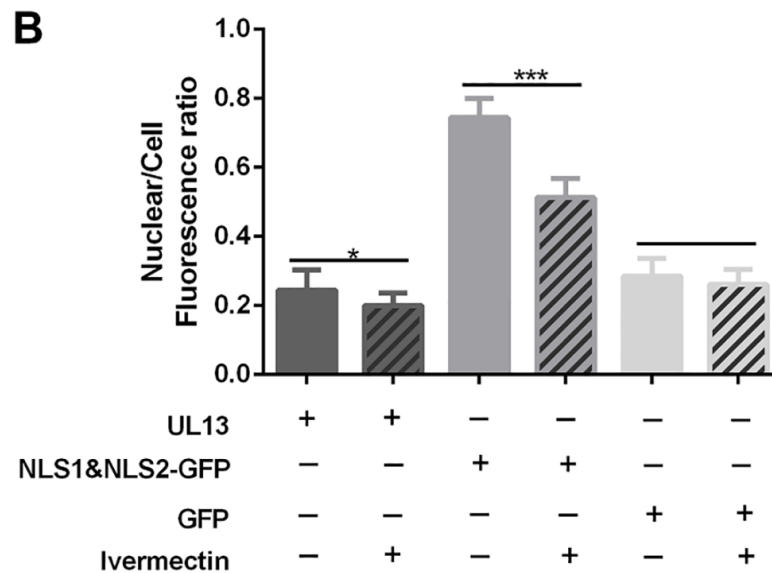
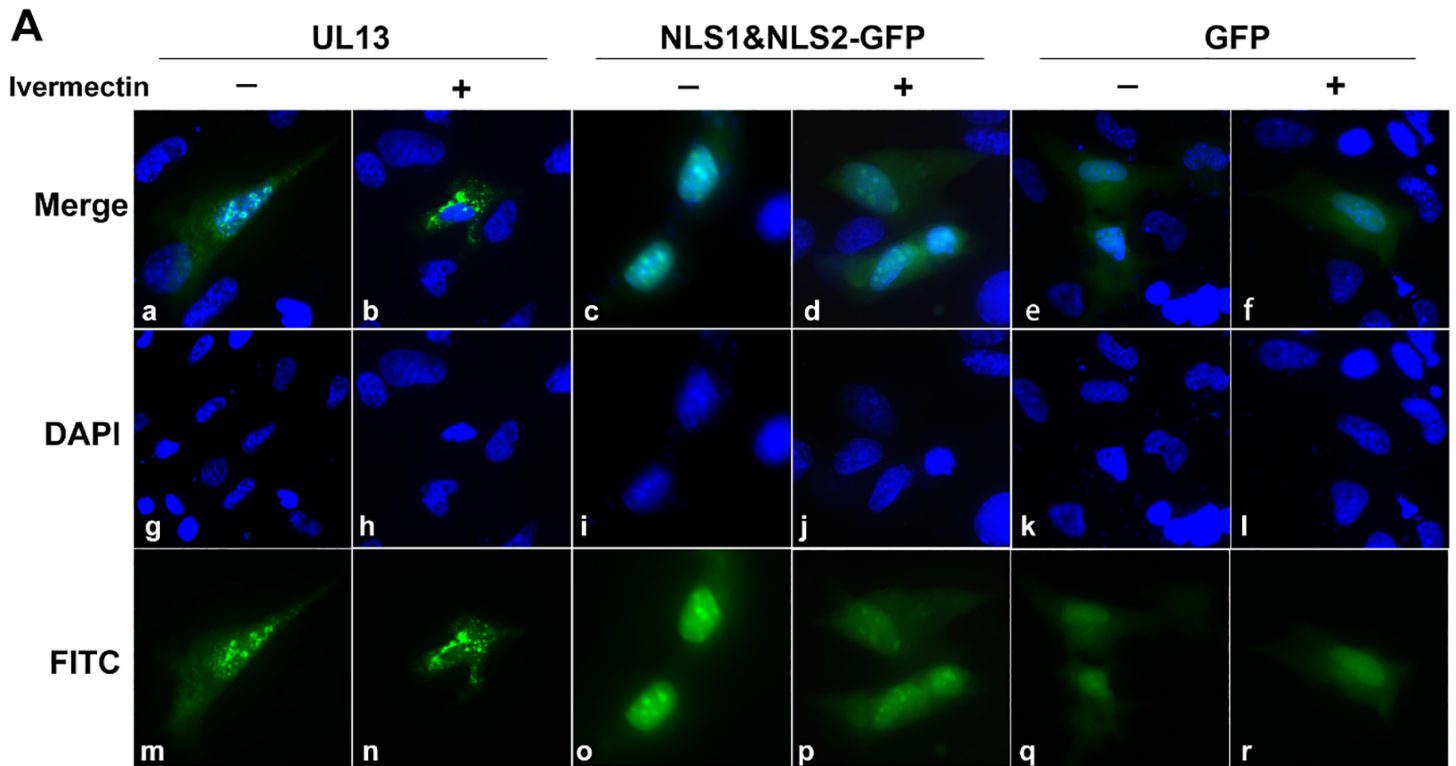


**Figure 3**

The effect of nuclear import inhibitors on the location of DEV pUL13 assay. (A) Location of UL13-GFP/ NLS1&NLS2-GFP protein with or without ivermectin treatment. At 16h post transfection, 25  $\mu$ M ivermectin was added 1 h before fixation. Images of the GFP reporter (green) and nuclei stained with DAPI (blue) were recorded in separate channels using a  $\times 40$  objective and merged in SPOT software. (B) Comparison of the nuclear and cytoplasmic fluorescence ratio between protein with or without ivermectin treatment. Mean nuclear and cytoplasmic fluorescence ratio was quantified using Image-Pro Plus software; analysis of the differences in the nuclear and cytoplasmic fluorescence ratio of UL13-GFP/ NLS1&NLS2-GFP protein with or without ivermectin treatment was performed using ANOVA with GraphPad Prism 6.0 software. N=50 for each group.

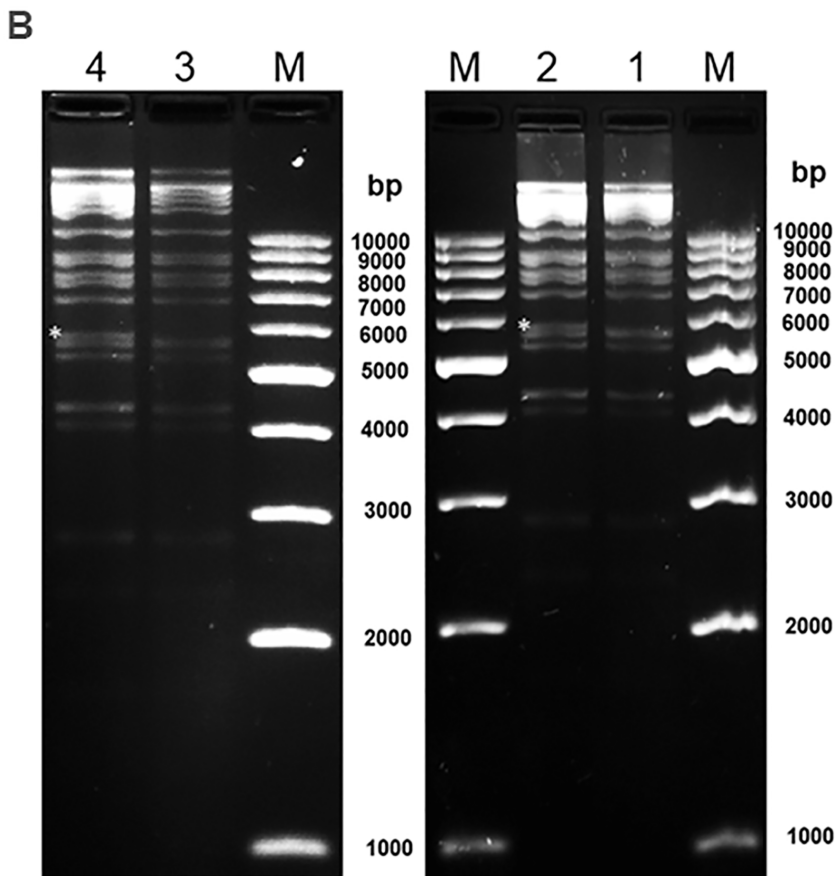
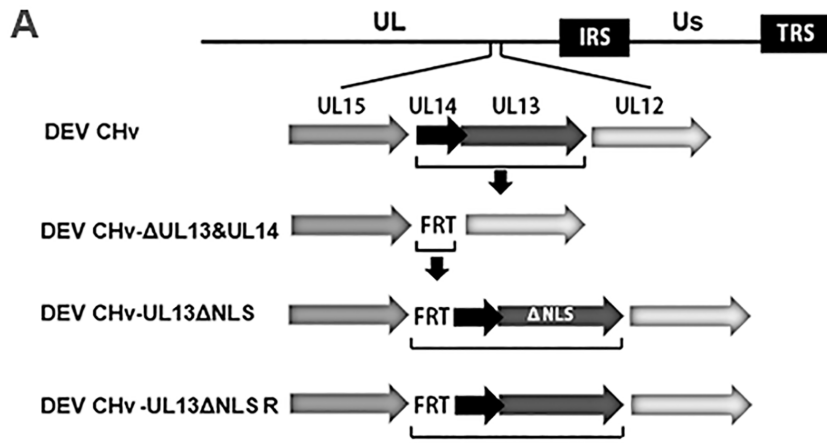


**Figure 4**

Construction and identification of DEV CHv- $\Delta$ UL13 and DEV CHv- $\Delta$ UL13R recombinant viruses. (A) Schematic representation of the DEV genome in the UL13 region and part of the sequence for DEV CHv-UL13 $\Delta$ NLS and the repaired DEV CHv-UL13 $\Delta$ NLS R. (B) RFLP analysis. Lane 1 and lane 3, DEV CHv -G plasmids were digested with *Sall* restriction endonuclease; Lane 2, DEV CHv-UL13 $\Delta$ NLS-G plasmids were digested with *Sall* restriction endonuclease; Lane 4, DEV CHv-UL13 $\Delta$ NLS R-G plasmids were digested with *Sall* restriction endonuclease. Digestion of the deletion and revertant products caused the size of the 5,714 bp fragment of the parental virus (Lane 1 and lane 3) to change to 5,765 bp and 5,798 bp (Lane 2 and Lane 4), respectively. No extraneous alterations were evident in either clone. M, 1 kb plus DNA ladder. \*: Different band.

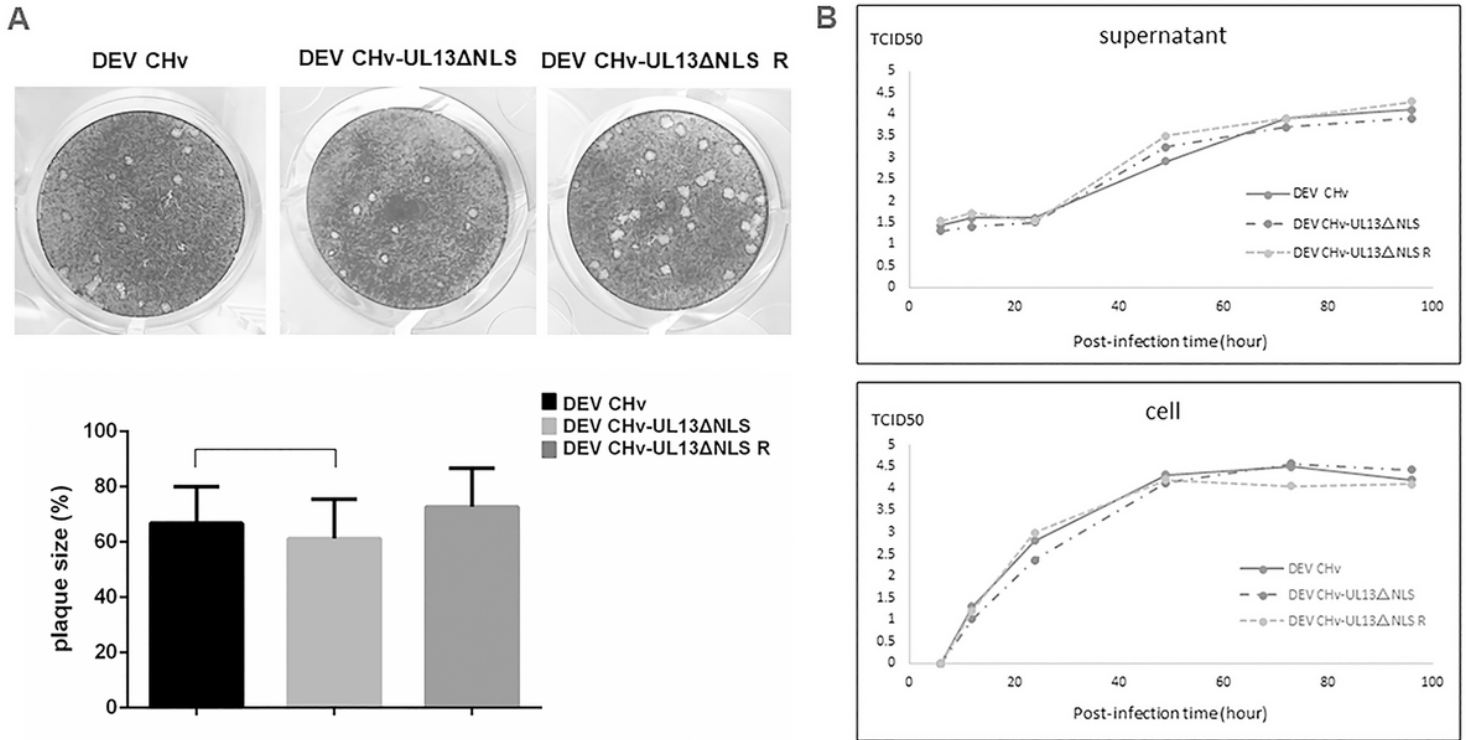


**Figure 5**

Analysis of the characteristics of the UL13-deletion mutant virus in cell culture. (A) Plaque assay. The upper figures represent the phenotypes of the plaques formed by DEV CHv, DEV CHv-UL13ΔNLS, and DEV CHv-UL13ΔNLS R virus infection; the lower figure shows the analysis of the mean areas of the viral plaques formed by the various viruses during infection. The digital images were analyzed using Image-Pro Plus software and the statistical analyses were performed using GraphPad Prism 6.0 software. (B) Growth curve. DEF were infected with DEV CHv, DEV CHv-UL13ΔNLS, and DEV CHv-UL13ΔNLS R at a titer of 200 TCID<sub>50</sub> and harvested at 6, 12, 24, 48, 72, and 96 h post infection. The curves were generated based on the titers of the different harvests, by testing for the TCID<sub>50</sub> using Excel. And the significant difference analyses between DEV CHv and DEV CHv-ΔUL13 were performed using GraphPad Prism 6.0 software.

## Supplementary Files

This is a list of supplementary files associated with this preprint. Click to download.

- [Supplementarydatas.docx](#)